Green Chemistry

ROYAL SOCIETY OF CHEMISTRY

COMMUNICATION

View Article Online
View Journal | View Issue

Cite this: *Green Chem.*, 2021, **23**, 1609

Received 10th November 2020,
Accepted 14th January 2021

DOI: 10.1039/d0gc03809a

rsc.li/greenchem

(Hexamethylbenzene)Ru catalysts for the Aldehyde-Water Shift reaction†

Alexander S. Phearman, [a,b] Jewelianna M. Moore, [a] Dayanni D. Bhagwandin, [b,c] Jonathan M. Goldberg, [b] D. Michael Heinekey [b] and Karen I. Goldberg *[a,b]

The Aldehyde-Water Shift (AWS) reaction uses H_2O as a benign oxidant to convert aldehydes to carboxylic acids, producing H_2, a valuable reagent and fuel, as its sole byproduct. (Hexamethylbenzene)Ru^{II} complexes are demonstrated to have higher activity and selectivity (up to 95%) for AWS over disproportionation than previously reported catalysts.

Introduction

Carboxylic acids are widely used in the production of consumer products, including polymers, esters, and amides. Carboxylic acids are commonly synthesized using stoichiometric harsh oxidants such as permanganate, chromate, or chlorite, although sometimes milder oxidants such as H_2O_2 or O_2 are used.[1–5] These latter two oxidants are also more atom efficient, reducing waste production. Another attractive synthetic route uses H_2O as the oxidant, and has been termed the "Aldehyde-Water Shift" (AWS, Scheme 1a) due to its similarity to the water gas shift reaction.[6] In addition to using a cheap, readily available, and benign oxidant, formation of a carboxylic acid by the AWS is accompanied by release of H_2, a valuable coproduct.

In the early 1980's, while investigating aldehyde disproportionation into carboxylic acid and alcohol under neutral or strongly basic conditions (Cannizzaro reaction), Maitlis noted that a Ru-catalyzed reaction afforded significantly more carboxylate than alcohol, while Ir- and Rh-complexes gave the expected 1 : 1 ratio.[7,8] A 1987 Murahashi study examining the dehydrogenation of aldehydes and alcohols to generate esters and lactones also reported that carboxylic acids formed when water and a hydrogen acceptor were present with $RuH_2(PPh_3)_4$ as a catalyst (up to 91% yield of butyric acid from butyraldehyde at 180 °C).[9] In the absence of a hydrogen acceptor, esters were formed preferentially and H_2 was not detected. In 2004, Stanley reported a dinuclear rhodium catalyst for tandem hydroformylation and AWS.[6] While activity was high (TOF ≈ 1900 h^{-1}) and heptanoic acid was the only observed product, the reaction required a CO headspace purge to prevent catalyst decomposition and remove H_2.[10]

More recently, Boncella demonstrated the use of a first-row transition metal complex, ($^{iPr}PN^HP$)$Mn(CO)_2(OH)$ ($^{iPr}PN^HP$ = (HN-{$CH_2CH_2(P^iPr_2)$}$_2$), to promote the AWS reaction, however strong product inhibition prevented catalytic turnover.[11] A variety of supported Cu, Pt, and Au catalysts have also been investigated for heterogeneous AWS reactivity in flow reactors, with up to 75% acid selectivity reported.[12] The AWS reaction has also been invoked as the second step of acceptorless alcohol dehydrogenation of primary alcohols to carboxylic acids or carboxylates.[13–20]

Our initial studies of catalysts for the AWS reaction focused on a series of Ir, Rh, and Ru half-sandwich complexes.[21] While Ir and Rh complexes were significantly more active as catalysts than the Ru compounds, their selectivity for carboxylic acid product was low and the competing aldehyde disproportionation reaction (Scheme 1b) dominated. While aldehyde dispro-

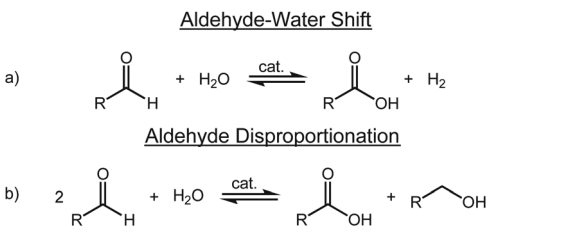

Scheme 1 (a) The Aldehyde-Water Shift reaction and (b) aldehyde disproportionation under neutral conditions.

[a]*Department of Chemistry, University of Pennsylvania, 231 South 34th Street, Philadelphia, PA 19104, USA. E-mail: kig@sas.upenn.edu*
[b]*Department of Chemistry, University of Washington, Box 351700, Seattle, WA 98195-1700, USA*
[c]*Department of Chemistry, Hunter College CUNY, 695 Park Avenue, New York, NY 10065, USA*

†Electronic supplementary information (ESI) available. CCDC 2034882 (**9**). For ESI and crystallographic data in CIF or other electronic format see DOI: 10.1039/d0gc03809a

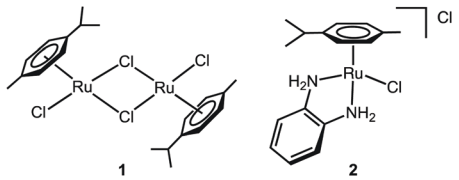

Chart 1 Best *p*-cymene supported ruthenium complexes previously screened for the AWS.

portion does produce carboxylic acid, the maximum yield is 50%, as it also produces an equivalent of alcohol. This initial study prompted further investigation into a series of (*p*-cymene)Ru complexes bearing different bidentate ligands with the goal of increasing the activity of the more selective Ru catalysts.[22] It was determined that the use of the catalyst precursor $[(\eta^6\text{-}p\text{-cymene})RuCl_2]_2$ dimer (**1**) and complexes with chelating bidentate amine ligands such as $[(\eta^6\text{-}p\text{-cymene})Ru(o\text{-PDA})Cl]Cl$ (**2**) (*o*-PDA = *ortho*-phenylenediamine) (Chart 1) resulted in improved activity while maintaining good selectivity using acetaldehyde as a substrate in aqueous solution (*e.g.* 92% conversion and 85% acid selectivity after 20 h submerged in a 105 °C oil bath). The only other product observed was ethanol, formed from aldehyde disproportionation.

It was postulated that the selectivity-determining step in the catalytic cycle was the reaction of a M–H intermediate with either H^+ or aldehyde. The subsequent development of an aqueous hydricity scale by the Miller group[23] revealed an interesting correlation between M–H hydricity and the AWS selectivity observed with Ir, Rh and Ru catalysts. Complexes that exhibited low AWS selectivity (Cp*Ir and Cp*Rh, Cp* = pentamethylcyclopentadienyl) were characterized as less hydridic than the corresponding (*p*-cymene)Ru complexes, which exhibited higher AWS selectivity. While it is unclear if the thermodynamic hydricity is a crucial factor for selectivity, this empirical observation motivated us to test more hydridic Ru complexes for the AWS reaction. Specifically, we examined more electron-donating $(\eta^6\text{-}C_6Me_6)Ru$ complexes, as $[(\eta^6\text{-}C_6Me_6)Ru(2,2'\text{-bipyridine})H]^+$ proved to be the most hydridic complex of the complexes studied by Miller and coworkers.[23]

Herein, we report the use of $(\eta^6\text{-}C_6Me_6)Ru$ complexes to enable highly selective catalytic conversion of aldehydes to carboxylic acids by the Aldehyde-Water Shift reaction with low catalyst loadings of 0.4 mol%. The use of these complexes resulted in improved activity along with the best AWS selectivity to date of any reported catalytic system. Results of catalysis using a variety of bidentate ligands, as well as selectivity dependence on H_2 pressure and pH further contribute to the understanding of this reaction pathway.

Results and discussion

Informed by our previous work, initial studies focused on $[(\eta^6\text{-}C_6Me_6)RuCl_2]_2$ (**3**) and $[(\eta^6\text{-}C_6Me_6)Ru(o\text{-PDA})Cl]Cl$ (**4**) (Chart 2; Table 1, entries 1–4). Complete conversion of acetaldehyde in

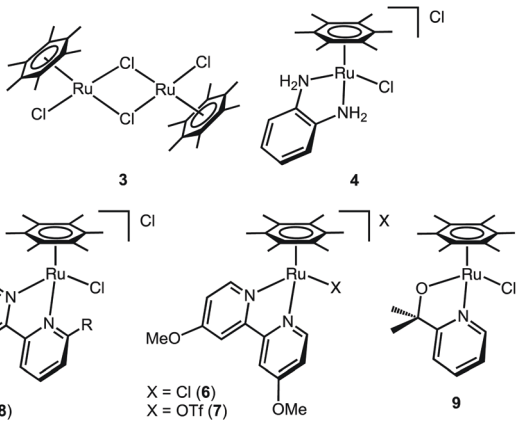

Chart 2 Hexamethylbenzene-supported ruthenium complexes screened for AWS reactivity in this study.

Table 1 Comparison of precatalyst performance for acetaldehyde oxidation

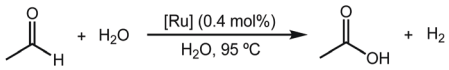

Entry	Precatalyst	Time (h)	Acid yield (%)	Alcohol yield (%)	Acid selectivity (%)
1	**3**	3	68(7)	3.8(8)	94.3(2)
2	**3**	5	83(2)	4.8(7)	94.6(9)
3	**4**	3	55.1(6)	2.7(1)	95(1)
4	**4**	5	75(8)	6(1)	93(1)
5	**5**	5	0.5(1)	0	100
6	**5**	50	4.2	3.1	57.3
7	**6**	5	1.2(3)	0	100
8	**7**	5	0.8(2)	0	100
9	**8**	5	10.8	6.6	61.9
10	**9**	5	53.4(12)	16.5(10)	76.4(15)

Reaction conditions: 5 mL H_2O, 2.5 mmol acetaldehyde, 0.2 mol% dimeric precatalyst or 0.4 mol% monomeric precatalyst, 95 °C, N_2 atmosphere. Quantification was by ^1H NMR spectroscopy using phenol as internal standard and data with standard deviations (contained in parentheses) were repeated in at least triplicate.

aqueous solution was observed after 20 hours at 105 °C[24] in the presence of either **3** or **4**, with >95% selectivity for acetic acid. Production of hydrogen was confirmed by GC-TCD (Fig. S3†). Since full conversion was achieved under these conditions, further experiments were carried out at lower temperature and with shorter reaction times to assess differences in activity between catalysts. When the temperature was lowered to 95 °C and the reaction time was limited to 5 h, **3** and **4** achieved 88 and 81% conversion of acetaldehyde to acetic acid with selectivities of 95 and 93%, respectively (Table 1, entries 2 and 4). In contrast, the *p*-cymene complex **2** required 20 h at 105 °C to reach similar conversions with only 85% selectivity for the acid product.[22]

Despite Miller's report of $[(\eta^6\text{-}C_6Me_6)Ru(2,2'\text{-bipyridine})H]^+$ being the most hydridic of the complexes they analyzed, hydricity doesn't appear to be the only important parameter for the

AWS reaction, as various monomeric (η^6-C_6Me_6)Ru complexes bearing substituted bipyridine ligands (**5–8**) showed very little activity (Table 1, entries 5–9). For example, even after 50 h reaction times, <8% conversion was observed with precatalyst **5** (Table 1, entry 6). Use of the more electron donating 4,4′-dimethoxy-2,2′-bipyridine ligand (precatalyst **6**) only resulted in 1.2% acid yield after 5 hours at 95 °C (Table 1, entry 7). Exchanging the inner- and outer-sphere chlorides of **6** for weakly coordinating triflate anions (**7**) had no effect (Table 1, entry 8). The hydroxyl groups of the 6,6′-dihydroxy-2,2′-bipyridine have previously been suggested to participate in bifunctional catalysis, and Ru and Ir half sandwich catalysts bearing this ligand have been shown to catalyze transfer hydrogenation,[25] CO_2 reduction,[26] alcohol dehydrogenation,[27–30] and water splitting.[31] In the AWS reaction of acetaldehyde, complex **8**, which bears this hydroxy substituted bipyridine, mainly facilitated disproportionation, resulting in only 62% selectivity for acetic acid with 17% conversion (Table 1, entry 9). A new (η^6-C_6Me_6)Ru complex supported by a pyridine alkoxide ligand, (η^6-C_6Me_6)Ru(2-(2′-pyridyl)-2-propanoate)Cl (**9**), was synthesized to test the effect of a monoanionic bidentate ligand on the AWS reaction (Scheme 2). Characterization of **9** by X-ray diffraction (Fig. S8†) shows that the complex has the expected three-legged piano stool structure with the pyridine alkoxide ligand coordinated in a bidentate fashion. As a catalyst for AWS with acetaldehyde, **9** afforded acetic acid in 53.4% yield (5 h at 95 °C), but with an acid selectivity of only 76% (Table 1, entry 10).

Substrate scope

Previously-studied half sandwich complexes for the AWS reaction exhibited high acid selectivity for only linear aldehydes. Using benzyl and branched alkyl aldehydes as substrates resulted in greatly reduced conversion and acid selectivity. A brief substrate scope using complex **3** was investigated. A less polar solvent system, 70 : 30 H_2O : 1,4-dioxane, was used to improve substrate solubility and eliminate potential biphasic reaction mixtures. A longer reaction time of 20 h at 95 °C was also employed to achieve appreciable conversions.[32]

Overall, the increased steric bulk of isobutyraldehyde and pivaldehyde resulted in decreased catalyst activity and selectivity relative to acetaldehyde. Isobutyraldehyde was converted with 87% selectivity to isobutyric acid (79% conversion), while pivaldehyde was converted with 76% selectivity (37% conversion, Table 2, entries 2–3). The selectivity and conversion for benzaldehyde was very similar to that of pivaldehyde at 80% and 33%, respectively.[33] While there is less steric bulk close to the carbonyl group for benzaldehyde, the phenyl ring conjugation renders the α-carbonyl carbon less electrophilic. While less impressive than the results for the AWS with acetaldehyde, these results are marked improvements over the reactions carried out with the *p*-cymene-supported **2** as the precatalyst for these substrates. Even under more forcing conditions (105 °C), the *p*-cymene-supported **2** resulted in only 5% conversion of pivaldehyde and <1% conversion of benzaldehyde in the same time.[22]

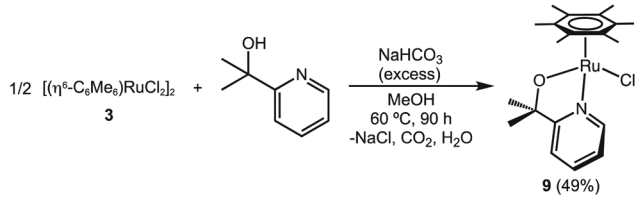

Scheme 2 Synthesis of (η^6-C_6Me_6)Ru(2-(2′-pyridyl)-2-propanoate)Cl (**9**).

Table 2 Substrate scope studied for aldehyde oxidation

Entry	Substrate	Acid yield (%)	Alcohol yield (%)	Acid selectivity (%)
1[a]		83(2)	4.8(7)	94.6(9)
2		69(2)	10(1)	87(1)
3		27.8(13)	8.7(5)	76.0(4)
4		26.3(5)	6.5(2)	80.3(3)
5[b]		13.3(2)	1.9(1)	87.6(4)
6[b,c]	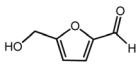	7	—	100

Reaction conditions: 3.5 mL H_2O, 1.5 mL 1,4-dioxane, 2.5 mmol substrate, 0.005 mmol **3**, 95 °C, 20 h, N_2 atmosphere. Reaction products were quantified by GC-FID. All experiments were repeated in at least triplicate with standard deviation provided in parentheses. [a] Reaction run in 100% H_2O for 5 h and products were quantified by ^{1}H NMR spectroscopy. [b] Reaction run in 50 : 50 H_2O : 1,4-dioxane. [c] Quantitative $^{13}C\{^1H\}$ NMR analysis using inverse-gated pulse sequence to determine yield and selectivity.

trans-Cinnamaldehyde was also used as a substrate to test the tolerance of internal alkene functionalities to AWS conditions, including H_2 formation (Scheme 3). Although conversion was low after 20 hours, *trans*-cinnamic acid was the major product (5.9% yield) when **3** was used as the catalyst at 95 °C in 70 : 30 H_2O : 1,4-dioxane solvent. The saturated carboxylic acid, 3-phenylpropanoic acid, was also observed in 3.6% yield,

Renewable substrates furfural and hydroxymethylfurfural (HMF), which are derived from the dehydration of sugars, have been extensively studied as bio-based platform chemicals.[34,35] When furfural was used as the substrate with catalyst **3** (50 : 50 H_2O : 1,4-dioxane, 20 h, 95 °C), high selectivity of 88% for oxidation was observed, albeit in low yield (13% furanoic acid) (Table 2, entry 5). Using the same conditions with HMF,[36] clean conversion to hydroxymethylfuroic acid (7% yield) was observed (Table 2, entry 6). No competing oxidation of the alcohol moiety was observed under these reaction conditions, demonstrating selectivity for aldehyde groups over alcohols under mild conditions.

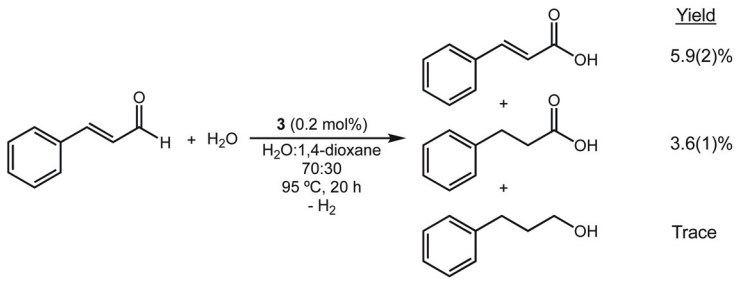

Scheme 3 Oxidation of cinnamaldehyde using **3**. Standard deviation in parentheses.

indicating that the internal alkene can act as an intramolecular hydrogen acceptor. Only trace 3-phenylpropanol was observed and the direct product of aldehyde disproportionation, cinnamyl alcohol, was not detected by GC. Formation of the saturated carboxylic acid is perhaps not surprising as transfer hydrogenations using (η^6-arene)Ru complexes have been well-studied.[37,38] In addition, when Murahashi studied the reaction of water with crotonaldehyde, another α,β-unsaturated substrate, the saturated carboxylic acid was produced in 75% selectivity after 24 hours at 180 °C with $RuH_2(PPh_3)_4$.[9] The results with catalyst **3** can be compared to those obtained with the *p*-cymene catalyst, [(η^6-*p*-cymene)Ru(*o*-PDA)Cl][Cl] (**2**) where no cinnamaldehyde conversion was observed after 20 h at 105 °C.[22]

Time-dependent selectivity

Monitoring the conversion of benzaldehyde to benzoic acid and benzyl alcohol by **3** at 95 °C in 70 : 30 H_2O : 1,4-dioxane over time revealed a clear time-dependent selectivity profile (Fig. 1, Table S2†). The background disproportionation reaction remains constant over 40 h as evidenced by the steadily increasing and linear benzyl alcohol yield with respect to time (blue circles, linear fit R^2 = 0.998). In contrast, the benzoic acid yield initially rises rapidly before the slope (Δbenzoic acid yield/Δtime) decreases (red triangles). As benzoic acid is produced through both the AWS reaction and aldehyde disproportionation, we subtracted the amount of benzoic acid produced through disproportionation (*i.e.* subtracted the amount of benzyl alcohol produced as each are generated in a 1 : 1 ratio during disproportionation) to more clearly visualize the change in AWS reactivity over time. As demonstrated through the subtraction of benzoic acid produced *via* disproportionation (green open triangles, Fig. 1), AWS has essentially stopped after ~20 h. Furthermore, the linear increase in the alcohol yield also supports that alcohol production is solely a product of transfer hydrogenation (disproportionation) and not hydrogenation with H_2 produced from the AWS reaction under these conditions. If hydrogenation played a significant role, the slope of the alcohol yield would be expected to change over time as H_2 production from the AWS reactions slows to near zero at 20 h.

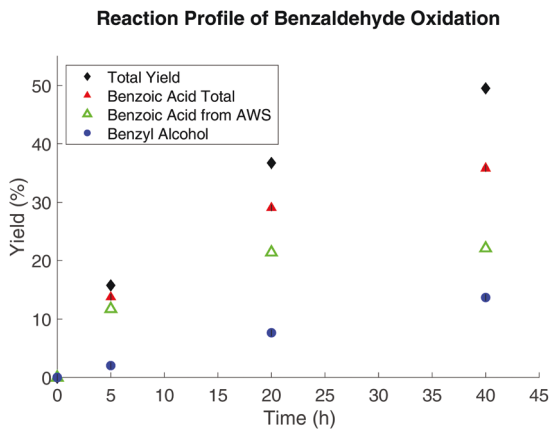

Fig. 1 Time-dependent selectivity profile for benzaldehyde oxidation. Reaction conditions: 3.5 mL H_2O, 1.5 mL 1,4-dioxane, 2.5 mmol benzaldehyde, 0.005 mmol **3** (0.2 mol%), 95 °C, N_2 atmosphere. Quantified by GC-FID. All entries repeated in at least triplicate. Yields in tabular format can be found in Table S2.†

We considered two possibilities for the decrease in AWS reaction over time. First, because the AWS reaction produces carboxylic acid product, the pH of the reaction solution decreases with higher conversion. Several protonation and deprotonation events occur throughout the proposed catalytic cycle, including the proposed selectivity-determining step (see later discussion). Second, the released hydrogen builds up in the reaction vessels over time. Thus, the increased H_2 pressure could inhibit the AWS pathway.

To examine the effect of pH on the reaction, we attempted to study the catalytic reactions at constant pH by using sodium phosphate buffered solutions (0.25 M, pH 6.0 or 7.0). Unfortunately, the mass balance of products and starting material was consistently low (70–90%) for these reactions after workup, making any conclusions based on these experiments suspect.[39] A different strategy to investigate the role that the increased concentration of benzoic acid and lower pH might have on the AWS reaction was then employed. Experiments were carried out with benzoic acid added to the starting solution. Thus, 5 or 25 mol% benzoic acid (0.125 or 0.625 mmol) relative to substrate was added to the standard 2.5 mmol benzaldehyde loading and the reaction progress was measured after 20 h at 95 °C in 70 : 30 H_2O : 1,4-dioxane. The amount of additional acid (greater than the original 0.125 or 0.625 mmol) was recorded (Table 3). In general, increasing

Table 3 Effect of added benzoic acid on oxidation of benzaldehyde

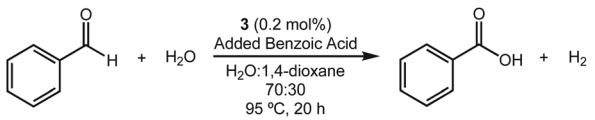

Added benzoic acid (mol%)	Benzoic acid yield (additional, %)	Benzyl alcohol yield (%)	Acid selectivity (%)
0	26.3(5)	6.5(2)	80.3(3)
5	17.2(14)	4.3(1)	80.0(9)
25	14.9(4)	4.4(3)	77.2(14)

Reaction conditions: 3.5 mL H_2O, 1.5 mL 1,4-dioxane, 2.5 mmol benzaldehyde, 0.005 mmol **3** (0.2 mol%), added benzoic acid as shown in table, 95 °C, 20 h, N_2 atmosphere. Reaction products were quantified by GC-FID. Experiments were repeated in triplicate with standard deviation in parentheses.

amounts of added benzoic acid led to lower consumption of benzaldehyde after 20 h. Although both AWS and disproportionation are inhibited by the addition of benzoic acid, as can been seen in the experiments with 5 mol% and 25 mol% added benzoic acid, the AWS experiences a slightly greater inhibition than disproportionation.

Likewise, the effect of H_2 pressure on the Aldehyde-Water Shift was investigated. To determine the effect of H_2 pressure, reactions were performed in a side-by side fashion, one in the normal closed system and the other with a vent needle to an outlet bubbler. The outlet tubing to the bubbler was purged thoroughly with N_2 immediately before use to prevent introduction of O_2 into the reaction.[40] To study H_2 dependence, a moderately lower reaction temperature (85 °C) was used to minimize solvent loss. This experimental design was carried out in triplicate at both 20 and 70 h reaction times. The selectivity for benzoic acid in the open system was significantly higher after both 20 and 70 h, confirming that H_2 pressure inhibits the AWS reaction (Table 4). This result is consistent with the work of Stanley and co-workers, who demonstrated

Table 4 Effect of hydrogen pressure release

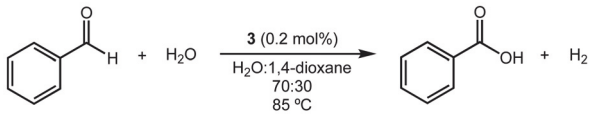

	Time (h)	Acid yield (%)	Alcohol yield (%)	Total yield (%)	Acid selectivity (%)
Vented	20	15.2(12)	1.4(1)	16.6(12)	91.3(8)
Vented	70	27.9(7)	3.4(4)	31.3(8)	89.3(12)
Closed	20	18.1(8)	3.5(2)	21.6(8)	84.0(3)
Closed	70	25.6(8)	7.6(5)	33.2(9)	77.1(6)

Reaction conditions: 3.5 mL H_2O, 1.5 mL 1,4-dioxane, 2.5 mmol benzaldehyde, 0.005 mmol **3** (0.2 mol%), 85 °C. Reaction products were quantified by GC-FID. Experiments were repeated in triplicate with standard deviation in parentheses.

that purging the reaction headspace of their system with CO increased AWS selectivity.[6] In addition, within error, acid selectivity in the vented experiments does not change at the 20 and 70 h timepoints, while it decreases from 84.0(3) to 77.1(6) in a closed system, further demonstrating the benefit of releasing H_2 pressure on acid selectivity.

Proposed catalytic cycle

The proposed catalytic cycle in Scheme 4 is based on mechanistic proposals for similar acceptorless alcohol dehydrogenation reactions,[14,18,29,41] as well as computational studies carried out by the Cundari group.[21,42] The cycle is depicted with a generic monodentate half-sandwich complex, as the speciation of **3** under catalytic conditions is unknown and different species bearing the (η^6-C_6Me_6)Ru manifold may share a common reactive intermediate.

Dissociation of a ligand from the precatalyst (**A**) generates an unsaturated Ru complex (**B**) (Scheme 4). Activation of an aldehyde by coordination to Ru (**C**) facilitates nucleophilic attack by H_2O and tautomerization to give a *gem*-diol (**D**). With some substrates, significant amounts of *gem*-diol are present in aqueous solutions, which could associate directly with **B** to form **D**. We note that substrates giving high conversion in this study form significant amounts of *gem*-diol in H_2O at neutral

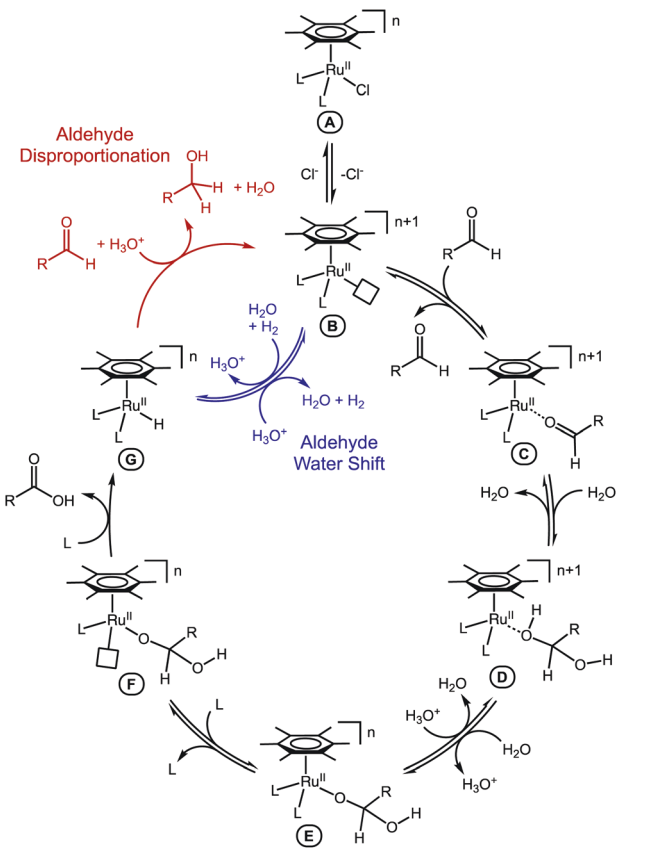

Scheme 4 Proposed catalytic cycle. Selectivity determining step highlighted in blue (AWS) and red (aldehyde disproportionation).

pH ($K_{hydration}$ = 1.25 for acetaldehyde),[43] while substrates giving low conversion exist primarily in the aldehyde form ($K_{hydration}$ = 0.01 for benzaldehyde and 0.25 for pivaldehyde).[44] Deprotonation of the *gem*-diol (**D**) then forms a Ru-alkoxide (**E**). This step would be inhibited by increasing acid concentration, consistent with the observed decrease in conversion with added acid (Table 3). Subsequent β-hydride elimination or dissociative β-hydride abstraction[45–48] results in a Ru–H (**G**) and the carboxylic acid product. The low activity of complexes **6–8**, which have strongly-bound bidentate ligands, suggests that an open site (**F**) is required, consistent with a β-hydride elimination pathway. Ligands such as (*o*-PDA, **4**) or Cl^- are likely labile enough to allow formation of **F**. Although not all of the complexes studied here have been crystallographically characterized, the *p*-cymene derivatives of **4–7** have been (Fig. S13†).[25,49–51] It is evident that the Ru–N bonds are significantly elongated with primary amine donors compared to bipyridine nitrogen donors, indicating that *o*-PDA is not as tightly bound to Ru and would be more likely than bipyridine to act as a hemilabile ligand.

Selectivity for the AWS *vs*. aldehyde disproportionation would then arise from the reactivity of the Ru–H (**G**) (Scheme 4, top left). Protonation of **G** would release H_2 and regenerate a $16e^-$ unsaturated Ru complex, **B**, to complete the cycle. Alternatively, hydride transfer to an aldehyde and subsequent protonation in acidic aqueous conditions would yield alcohol product, thereby formally hydrogenating an equivalent of aldehyde and completing the disproportionation pathway. The demonstrated increase in acid selectivity when H_2 pressure is allowed to escape is consistent with this proposal, as only the AWS pathway releases H_2 as a product. By Le Chatelier's principle, release of H_2 would be expected to change the selectivity in favor of the AWS, especially at later reaction times. Further improvements in selectivity could likely be achieved by purging the reaction headspace to remove H_2 rather than simply releasing H_2 pressure. The slight decrease in acid selectivity when additional benzoic acid is added (Table 3) may be due to differences in $[H^+]$ dependency in the selectivity-determining step or change in speciation of **3**.

Conclusions

The use of Ru half-sandwich complexes with more electron donating C_6Me_6 arene rings resulted in significant improvements in selectivity and activity compared to *p*-cymene analogues for the Aldehyde-Water Shift reaction. The use of H_2O as both the oxygen atom source and solvent is unique, and concomitant H_2 release results in an atom efficient process under mild reaction conditions (95 °C) with low catalyst loadings (0.4 mol% Ru). While the use of electron rich arene ligands boosts selectivity for AWS, strongly-bound bidentate ancillary ligands drastically decrease reactivity. This observation supports that ligand dissociation (allowing for β-hydride elimination) is a key step in the catalytic cycle, and so informs future precatalyst design and optimization. Furthermore, selectivity was demonstrated to be dependent on headspace H_2 pressure and catalyst activity is reduced with increasing acid concentration. This behavior is thus consistent with the "shift" nature of the AWS reaction. Overall our results demonstrate how an improved understanding of the AWS reaction can facilitate improvement in the reactivity and selectivity of catalysts for this relatively underdeveloped environmentally-friendly aldehyde oxidation method.

Conflicts of interest

There are no conflicts to declare.

Acknowledgements

The authors thank Dr. Louise M. Guard for helpful discussions and the group of Professor Robert Crabtree (Yale University) for the gift of 2-(2′-pyridyl)-2-propanol. Accurate mass measurement analysis was carried out by Dr. Charles W. Ross III (University of Pennsylvania) and X-ray crystallography was carried out by Dr. Patrick J. Carroll (University of Pennsylvania). This work was supported by the National Science Foundation under the CCI Center for Enabling New Technologies through Catalysis (CENTC) (CHE-1205189), the Department of Energy (DE-SC0018057), and the Penn Undergraduate Research Mentoring Program (J.M.M.). The NSF Major Research Instrumentation Program (NSF CHE-1827457, 400 MHz NMR spectrometer), the NIH supplemental awards 3R01GM118510-03S1 and 3R01GM087605-06S1 (600 MHz NMR spectrometer), and Vagelos Institute for Energy Science and Technology are recognized for their support of NMR instrumentation used in this study.

References

1 M. B. Smith and J. March, *March's Advanced Organic Chemistry: Reactions, Mechanisms and Structure*, John Wiley and Sons, Inc., Hoboken, NJ, 6th edn, 2007.
2 H. Yu, S. Ru, G. Dai, Y. Zhai, H. Lin, S. Han and Y. Wei, *Angew. Chem., Int. Ed.*, 2017, **56**, 3867–3871.
3 M. Liu and C.-J. Li, *Angew. Chem., Int. Ed.*, 2016, **55**, 10806–10810.
4 Y. Zhang, Y. Cheng, H. Cai, S. He, Q. Shan, H. Zhao, Y. Chen and B. Wang, *Green Chem.*, 2017, **19**, 5708–5713.
5 J. Kubitschke, H. Lange and H. Strutz, *Carboxylic Acids, Aliphatic. Ullmann's Encyclopedia of Industrial Chemistry*, 2014, pp. 1–18.
6 G. G. Stanley, D. A. Aubry, N. Bridges, B. Barker and B. Courtney, *Prepr. Pap. – Am. Chem. Soc., Div. Fuel Chem.*, 2004, **49**, 712–713.
7 J. Cook, J. E. Hamlin, A. Nutton and P. M. Maitlis, *J. Chem. Soc., Chem. Commun.*, 1980, 144–145, DOI: 10.1039/C39800000144.

8 J. Cook, J. E. Hamlin, A. Nutton and P. M. Maitlis, *J. Chem. Soc., Dalton Trans.*, 1981, 2342–2352, DOI: 10.1039/dt9810002342.
9 S. Murahashi, T. Naota, K. Ito, Y. Maeda and H. Taki, *J. Org. Chem.*, 1987, **52**, 4319–4327.
10 A. R. Barnum, Ph. D. Dissertation, Louisiana State University, 2012.
11 A. M. Tondreau, R. Michalczyk and J. M. Boncella, *Organometallics*, 2017, **36**, 4179–4183.
12 W.-C. Wen, S. C. Eady and L. T. Thompson, *Catal. Today*, 2020, **355**, 199–204.
13 N. Xiang, P. Xu, N. Ran and T. Ye, *RSC Adv.*, 2017, **7**, 38586–38593.
14 E. Balaraman, E. Khaskin, G. Leitus and D. Milstein, *Nat. Chem.*, 2013, **5**, 122–125.
15 R. E. Rodriguez-Lugo, M. Trincado, M. Vogt, F. Tewes, G. Santiso-Quinones and H. Grutzmacher, *Nat. Chem.*, 2013, **5**, 342–347.
16 J.-H. Choi, L. E. Heim, M. Ahrens and M. H. G. Prechtl, *Dalton Trans.*, 2014, **43**, 17248–17254.
17 K.-i. Fujita, R. Tamura, Y. Tanaka, M. Yoshida, M. Onoda and R. Yamaguchi, *ACS Catal.*, 2017, **7**, 7226–7230.
18 A. Sarbajna, I. Dutta, P. Daw, S. Dinda, S. M. W. Rahaman, A. Sarkar and J. K. Bera, *ACS Catal.*, 2017, **7**, 2786–2790.
19 R. Yamaguchi, D. Kobayashi, M. Shimizu and K.-i. Fujita, *J. Organomet. Chem.*, 2017, **843**, 14–19.
20 W. Yao, A. R. DeRegnaucourt, E. D. Shrewsbury, K. H. Loadholt, W. Silprakob, F. Qu, T. P. Brewster and E. T. Papish, *Organometallics*, 2020, **39**, 3656–3662.
21 T. P. Brewster, W. C. Ou, J. C. Tran, K. I. Goldberg, S. K. Hanson, T. R. Cundari and D. M. Heinekey, *ACS Catal.*, 2014, **4**, 3034–3038.
22 T. P. Brewster, J. M. Goldberg, J. C. Tran, D. M. Heinekey and K. I. Goldberg, *ACS Catal.*, 2016, **6**, 6302–6305.
23 C. L. Pitman, K. R. Brereton and A. J. Miller, *J. Am. Chem. Soc.*, 2016, **138**, 2252–2260.
24 Temperatures listed in this communication are that of a thermocouple-controlled hotplate and aluminum heating block. The heating block is half the height of the reaction vials.
25 I. Nieto, M. S. Livings, J. B. Sacci, L. E. Reuther, M. Zeller and E. T. Papish, *Organometallics*, 2011, **30**, 6339–6342.
26 S. Siek, D. B. Burks, D. L. Gerlach, G. Liang, J. M. Tesh, C. R. Thompson, F. Qu, J. E. Shankwitz, R. M. Vasquez, N. Chambers, G. J. Szulczewski, D. B. Grotjahn, C. E. Webster and E. T. Papish, *Organometallics*, 2017, **36**, 1091–1106.
27 G. Zeng, S. Sakaki, K.-i. Fujita, H. Sano and R. Yamaguchi, *ACS Catal.*, 2014, **4**, 1010–1020.
28 R. Zhu, B. Wang, M. Cui, J. Deng, X. Li, Y. Ma and Y. Fu, *Green Chem.*, 2016, **18**, 2029–2036.
29 R. Kawahara, K. Fujita and R. Yamaguchi, *Angew. Chem., Int. Ed.*, 2012, **51**, 12790–12794.
30 R. Kawahara, K. Fujita and R. Yamaguchi, *J. Am. Chem. Soc.*, 2012, **134**, 3643–3646.
31 J. DePasquale, I. Nieto, L. E. Reuther, C. J. Herbst-Gervasoni, J. J. Paul, V. Mochalin, M. Zeller, C. M. Thomas, A. W. Addison and E. T. Papish, *Inorg. Chem.*, 2013, **52**, 9175–9183.
32 The reported boiling point of a 70 : 30 water : 1,4-dioxane azeotrope is 88.2 °C at atmospheric pressure (E. R. Smith and M. Wojciechowski, *Journal of Research of the National Bureau of Standards*, 1937, **18**, 461–465). In a small volume (20 mL) sealed system the headspace pressure exceeds atmospheric pressure due to vapor pressure and the dihydrogen produced by the AWS, allowing the temperature of the solution to exceed 88.2 °C.
33 Papish and Brewster recently reported that a [(Cp*)Ir(6,6′-dihydroxy-2,2′-bipyridine)]$^{2+}$ complex is capable of decarbonylating benzoic acid (ref. 20). No evidence of decarbonylation is observed when complex **3** is used with benzaldehyde as substrate for the AWS reaction.
34 B. Saha and M. M. Abu-Omar, *Green Chem.*, 2014, **16**, 24–38.
35 A. A. Rosatella, S. P. Simeonov, R. F. M. Frade and C. A. M. Afonso, *Green Chem.*, 2011, **13**, 754–793.
36 Control reactions without Ru, showed that an aqueous solution of HMF, when heated to 95 °C for 20 h, resulted in a dark brown solution, while a 50 : 50 water : 1,4-dioxane mixture resulted in no color change.
37 T. Ikariya and A. J. Blacker, *Acc. Chem. Res.*, 2007, **40**, 1300–1308.
38 R. Noyori, *Angew. Chem., Int. Ed.*, 2002, **41**, 2008–2022.
39 In a mass balance control experiment with just benzaldehyde, buffer, and solvent, only 90% of the starting material was detected after workup.
40 In preliminary studies with acetaldehyde, it was noted that acid selectivity did not change greatly with reaction temperature (Fig. S11 and 12†).
41 T. Zweifel, J. V. Naubron and H. Grutzmacher, *Angew. Chem., Int. Ed.*, 2009, **48**, 559–563.
42 W. C. Ou and T. R. Cundari, *ACS Catal.*, 2014, **5**, 225–232.
43 J. L. Kurz, *J. Am. Chem. Soc.*, 1967, **89**, 3524–3528.
44 S. H. Hilal, L. L. Bornander and L. A. Carreira, *QSAR Comb. Sci.*, 2005, **24**, 631–638.
45 O. Blum and D. Milstein, *J. Organomet. Chem.*, 2000, **593–594**, 479–484.
46 N. A. Smythe, K. A. Grice, B. S. Williams and K. I. Goldberg, *Organometallics*, 2009, **28**, 277–288.
47 O. Blum and D. Milstein, *J. Am. Chem. Soc.*, 1995, **117**, 4582–4594.
48 C. M. Fafard and O. V. Ozerov, *Inorg. Chim. Acta*, 2007, **360**, 286–292.
49 T. Bugarcic, A. Habtemariam, R. J. Deeth, F. P. Fabbiani, S. Parsons and P. J. Sadler, *Inorg. Chem.*, 2009, **48**, 9444–9453.
50 X. Wu, J. Liu, D. Di Tommaso, J. A. Iggo, C. R. Catlow, J. Bacsa and J. Xiao, *Chem. – Eur. J.*, 2008, **14**, 7699–7715.
51 C. Aliende, M. Pérez-Manrique, F. A. Jalón, B. R. Manzano, A. M. Rodríguez and G. Espino, *Organometallics*, 2012, **31**, 6106–6123.